# X-Ray Intensity Fluctuation Spectroscopy Observations of Critical Dynamics in $Fe_3Al$

S. Brauer* and G. B. Stephenson
*IBM Research Division, T. J. Watson Research Center, P.O. Box 218, Yorktown Heights, New York 10598*

M. Sutton, R. Brüning, and E. Dufresne
*Center for the Physics of Materials and Department of Physics, McGill University, Montréal, Québec, Canada, H3A 2T8*

S. G. J. Mochrie
*Department of Physics, Massachusetts Institute of Technology, Cambridge, Massachusetts 02139*

G. Grübel, J. Als-Nielsen,† and D. L. Abernathy
*European Synchrotron Radiation Facility, B.P. 220, F-38043 Grenoble Cedex, France*
(Received 31 October 1994)

We have carried out intensity fluctuation spectroscopy measurements using coherent x rays to study the dynamics of critical fluctuations in a binary alloy at equilibrium. An intense coherent hard x-ray beam, produced from an undulator source, was scattered from a single crystal of $Fe_3Al$ held at temperatures near the $B2$-$DO_3$ order-disorder transition. A speckle pattern was observed at the $(\frac{1}{2}\frac{1}{2}\frac{1}{2})$ superlattice reflection. Below $T_c$ it was essentially static, while above $T_c$ it fluctuated in time. The behavior of the normalized time correlation function is consistent with predictions of theory.

PACS numbers: 61.10.Lx, 05.40.+j, 42.30.Ms, 64.60.Ht

The development of techniques using coherent x rays is of considerable current interest. This is largely because new undulator-based synchrotron x-ray sources are capable of providing coherent hard x-ray beams several orders of magnitude more intense than previously available. In particular, several groups have been working to carry out intensity fluctuation spectroscopy (IFS) measurements using x rays [1]. This "XIFS" technique is especially promising because it should provide one of the few direct measurements of the dynamics of atomic-scale fluctuations. Observations of static speckle patterns in the scattering of coherent x rays from disordered systems have been reported as initial steps toward this goal [1–3]. In this Letter we report our first results using XIFS to measure the dynamics of order fluctuations in a metal alloy near its critical point.

To understand why XIFS is a probe of the dynamics of disorder, it is first necessary to understand the difference between scattering patterns produced by coherent and incoherent beams. When coherent light is scattered from a disordered system, it gives rise to a random diffraction or "speckle" pattern [4]. Such a speckle pattern is uniquely related to the *exact spatial arrangement* of the disorder. In contrast, if the incident beam is not coherent, the speckle is not resolved, and the scattering pattern is determined only by the *probability distribution* of the disorder.

Although the speckle pattern may be difficult to interpret as a spatial structure, a unique advantage in scattering with a coherent beam lies in the ability to observe the *dynamics* of the disorder. When the spatial arrangement of the disorder evolves with time, the speckle pattern also changes. The technique of IFS (also known as dynamic light scattering [5,6]) is simply the observation of the intensity fluctuations at a single point in the speckle pattern to obtain a direct measure of the dynamics. It is commonly used with visible coherent light to study processes such as the diffusion of micron-size particles in liquids. By instead using coherent hard x rays ($\lambda \sim 1$ Å) to conduct XIFS measurements, it should be possible to probe the dynamics of processes involving atomic length scales in a wide variety of materials. In contrast to conventional time-resolved x-ray scattering using an incoherent beam [7], XIFS could be used to study the dynamics of disorder in systems *at equilibrium*, where the exact arrangement of disorder evolves in time but its average distribution does not. In this work we introduce XIFS to study the dynamics of short-range order (SRO) fluctuations associated with a simple phase transition.

Our experiments were conducted at the undulator beam line 9 (Troika) of the European Synchrotron Radiation Facility. Figure 1 is a schematic of the apparatus. The nominal size of the undulator source is 0.21 mm × 0.97 mm (vert × horiz) full width at half maximum (FWHM), although slits located 27 m downstream from the source were used to restrict the effective horizontal

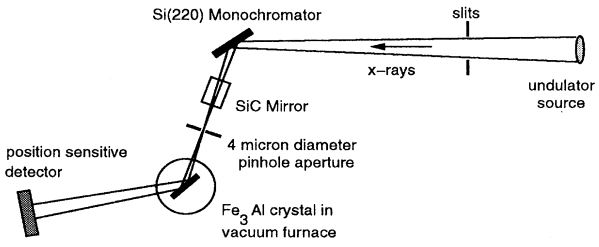


FIG. 1. Schematic of the experimental apparatus.

 0031-9007/95/74(11)/2010(4)$06.00 

source size to be equal to that in the vertical. X rays of wavelength $\lambda = 1.05$ Å and wavelength spread $\Delta\lambda/\lambda = 6 \times 10^{-5}$ were selected by a Si(220) monochromator, diffracting horizontally in the symmetric Bragg geometry. To suppress the harmonic content of the beam, a flat, vertically reflecting SiC mirror was placed downstream of the monochromator. Following the mirror a 4 $\mu$m diameter pinhole in a 50 $\mu$m thick platinum foil served as an x-ray aperture. In this geometry, the divergence of rays passing through the pinhole is determined by the source size $A = 0.21$ mm divided by the pinhole-to-source separation $R = 45$ m. For radiation passing through the pinhole, the transverse coherence length is $d_t = \lambda R/2A \simeq 11$ $\mu$m, so that the 4 $\mu$m pinhole selects a beam which is transversely coherent in both the vertical and horizontal. The flux through the pinhole was $5.7 \times 10^6$ photons per second at a typical storage ring current of 100 mA.

The single crystal we studied was slightly off-stoichiometric $Fe_3Al$ (27.1 at.% Al) [8], which has a continuous $B2$-$DO_3$ order-disorder transition with critical temperature $T_c$ near 824 K. This transition is analogous to a simple antiferromagnetic Ising model with a nonconserved order parameter (model $A$ dynamics [9]). The specimen was located as close to the pinhole as the sample vacuum furnace would permit (8 cm), in order to be within the near field of diffraction from the pinhole. The sample had a (110) surface normal and was oriented for the $(\frac{1}{2}\,\frac{1}{2}\,\frac{1}{2})$ superlattice reflection. The horizontally diffracted beam was observed with a Xe-$CO_2$ position-sensitive proportional counter. The detector was situated 3.64 m downstream from the specimen and masked by a 95 $\mu$m (26 $\mu$rad) high slit. For each detected photon, both the position and the arrival time were recorded. The 4096 position channels each corresponded to 13.5 $\mu$m (3.7 $\mu$rad) along the detector. The resolution of the detector was 149 $\mu$m (41 $\mu$rad), and the dark count rate was typically 0.003 counts per second per channel. The signal from a beam monitor located between the pinhole and the sample was used to normalize the data to variations in incident intensity.

In order to perfectly resolve a speckle pattern, the longitudinal coherence length $d_l = \lambda^2/2\Delta\lambda \simeq 1$ $\mu$m must exceed $2\mu \sin^2\theta$ for the symmetric reflection geometry [2]. Here $\theta = 9.02°$ is the scattering angle and $\mu = 15$ $\mu$m is the x-ray absorption length in the specimen, giving $2\mu \sin^2\theta \simeq 0.8$ $\mu$m. For the inclined geometry used here, the minimum $d_l$ is about twice as large. The wavelength spread $\Delta\lambda$ used was thus somewhat larger than ideal, and some loss of resolution of the speckle pattern occurred.

We first describe a typical speckle pattern observed with the sample well below $T_c$, in the long-range order (LRO) phase. At true equilibrium below $T_c$, the LRO domain size would have grown to equal the sample size; however, the domain coarsening process becomes increasingly slow as it proceeds, so that the sample typically contains a random arrangement of relatively static LRO domains [10].

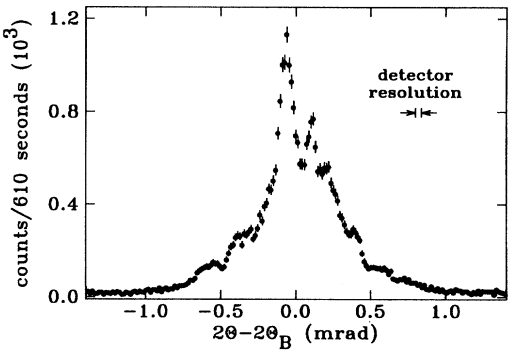


FIG. 2. The $(\frac{1}{2}\,\frac{1}{2}\,\frac{1}{2})$ superlattice peak in $Fe_3Al$ at $T = 803$ K, showing an imperfectly resolved x-ray speckle pattern. The detector channels have been binned by 4.

By appropriately cooling the sample from above $T_c$ over several hours, we prepared a domain distribution suitable for measuring a static speckle pattern. Figure 2 shows the $(\frac{1}{2}\,\frac{1}{2}\,\frac{1}{2})$ superlattice peak at $T = 803$ K, 21 K below $T_c$. The overall width of the peak (500 $\mu$rad) implies an average domain size of ~200 nm. The structure within the peak is an imperfectly resolved x-ray speckle pattern, formed because the two domain types introduce phase shifts to the scattered radiation which differ by $\pi$. The angular size of each "speckle" is expected to be equal to the FWHM of the Fraunhofer diffraction pattern of the pinhole itself, which we measured to be 27 $\mu$rad [1]. However, because of our 41 $\mu$rad detector resolution, we expect to measure features with a FWHM of ~50 $\mu$rad, which is in fair agreement with Fig. 2.

For the XIFS measurements, the sample was preannealed at $T = T_c - 2$ K for two days, so that the domain structure was well coarsened and essentially static. The observed superlattice peak FWHM was only ~70 $\mu$rad, or ~3 speckles, corresponding to an average domain size of 1.5 $\mu$m. To collect the XIFS data, the sample was heated to successively higher temperatures near $T_c$. At each point, the sample temperature was controlled to $\pm 0.05$ K, and the sample was allowed to equilibrate for about 1 h. The time-averaged peak intensity and resolution-corrected FWHM are shown in Fig. 3, as a function of temperature within $\pm 1$ K of $T_c$. There is a change in the slope of the intensity data and an abrupt increase in peak width at $T_c = 823.8$ K. Note that the count rate near $T_c$ is only about one count per second per speckle. Above $T_c$, the scattering persists owing to SRO fluctuations. The observed peak widths imply SRO correlation lengths $\xi$ of about 750 nm, although the time and volume averaged are too small to give accurate values of $\xi$. (We believe that this is the reason that the FWHM at 823.95 K exceeds that at 824.15 K.)

Figure 4 shows the scattered intensity averaged over 220 $\mu$rad (or about 8 speckles) centered on the superlattice peak, plotted as a function of time for each of five temperatures. The intensity is essentially constant below

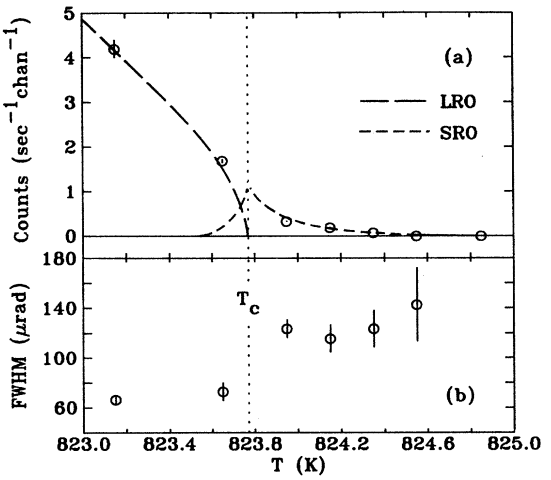


FIG. 3. The peak intensity (a) and overall width (b) of the $(\frac{1}{2}\frac{1}{2}\frac{1}{2})$ superlattice peak as a function of temperature. The dashed curves are guides to the eye indicating the LRO and SRO contributions to the scattering. The intensity was normalized to a ring current of 100 mA.

$T_c$ (upper 2 panels), where the signal is dominated by static LRO domains. The observed point-to-point deviations are quantitatively consistent with Poisson counting statistics (indicated by the $\pm 1\sigma$ error bars). This indicates that the source, optics, specimen, and detector meet the exacting stability requirements for an XIFS measurement. In contrast, intensity fluctuations of up to 30% relative amplitude are evident above $T_c$ (lower three panels), where the signal is due to SRO critical fluctuations. These are much larger in amplitude than the noise due to counting statistics, and there is a clear correlation between neighboring points. To our knowledge, these data constitute the first observation of the dynamics of equilibrium critical fluctuations at an alloy order-disorder transition.

The fluctuations can be quantified by the normalized time correlation function [11]

$$g^{(2)}(\tau) - 1 = \frac{\frac{1}{N}\sum_{i=0}^{N}[I(t_i) - \langle I\rangle][I(t_i + \tau) - \langle I\rangle]}{[\frac{1}{M}\sum_{i=0}^{M} I(t_i)]^2},$$

where $I(t_i)$ is the number of counts in the $i$th time-bin [12]. This function is nonzero when there are temporal fluctuations and zero when the signal is static. Figure 5 shows $g^{(2)}(\tau) - 1$ calculated from the data of Fig. 4, where the $\delta$-function contribution from counting statistics (based on the mean count rate) has been subtracted from the $\tau = 0$ point in each data set. A clear distinction can be seen in Fig. 5 between the static LRO signal observed below $T_c = 823.8$ K and the SRO fluctuations above $T_c$. At the two temperatures below $T_c$, the correlation functions are nearly zero. At the three temperatures above $T_c$, the correlation functions are nonzero, with amplitudes that are approximately equal and apparent correlation times of about 1000 s. However, because the observations typically span a time range of only 6000 s, these are not reliable estimates for the true correlation times, but instead only lower limits. Such long correlation times are not unreasonable near $T_c$ in this system. A crude estimate using $\tau_{\text{corr}} \approx \tau_0[(T - T_c)/T_c]^{-\nu z}$ with $\nu \approx \frac{2}{3}$, $z \approx 2$ [9], and a bare correlation time of $\tau_0 \approx 1$ s (based

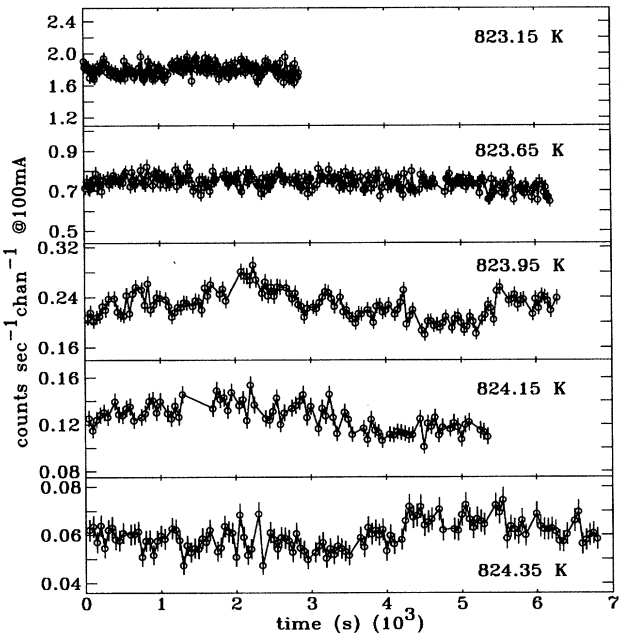


FIG. 4. The scattered intensity averaged over 220 $\mu$rad at the center of the superlattice peak, plotted as a function of time at various temperatures within $\pm 1$ K of $T_c$. To facilitate comparison, the data in each panel are plotted on the same scale relative to their mean intensity.

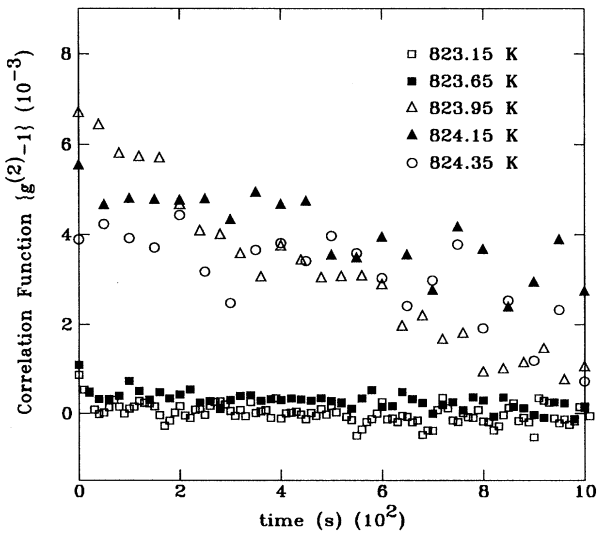


FIG. 5. Normalized time correlation function for the data shown in Fig. 4.

on reequilibration times well above and below $T_c$ [7]), gives $\tau_{\text{corr}} > 10^4$ s at the reduced temperatures used here.

From the theory of dynamic critical phenomena [9] it is straightforward to show [13] that $g^{(2)}(\tau)$ has universal properties near $T_c$ for a system of size $L > \xi$. In particular, the value of $g^{(2)}(\tau = 0) - 1$ at the position of the $(\frac{1}{2}\,\frac{1}{2}\,\frac{1}{2})$ LRO peak is expected to abruptly change from 2 above $T_c$ to 0 below $T_c$ [14]. In agreement with theory, our data for $g^{(2)}(\tau = 0) - 1$ show an abrupt change from a certain value above $T_c$ to nearly zero below; however, the value observed above $T_c$ is much smaller than 2. The value of 2 is expected when the speckle pattern is perfectly resolved and the time averages are carried out over periods long with respect to the correlation time. In our case, because of the low intensity we have summed the signal over many speckles, reducing fluctuation contrast and thus the observed value of $g^{(2)} - 1$. In addition, the time scale of our measurements may be smaller than the true correlation time, further reducing the observed value because of bias in the determination of $\langle I \rangle$. Experiments with longer counting times and improved intensity and resolution are underway in order to more accurately determine the behavior of $g^{(2)}(\tau)$ near $T_c$.

The authors would like to acknowledge S. Dierker, R. Fleming, R. Pindak, and I. K. Robinson for their assistance with the experiments and L. Berman for his assistance with preparatory experiments. The x-ray detector was kindly provided by M. Kocsis. Technical support from P. Feder and H. Gleyzolle is gratefully acknowledged. Discussions with G. Grinstein contributed significantly to the analysis. This work was supported in part by the NSERC of Canada and the Fonds FCAR of Québec. Work at MIT was supported by the NSF (Grant No. DMR 94-00334) and by the Michael and Philip Platzman Fund.

*Current address: Advanced Photon Source, Argonne National Laboratory, Argonne, IL 60439.

†Permanent address: Riso National Laboratory, DK 4000 Roskilde, Denmark.

[1] G. Grübel, J. Als-Nielsen, D. Abernathy, G. Vignaud, S. Brauer, G. B. Stephenson, S. G. J. Mochrie, M. Sutton, I. K. Robinson, R. Fleming, R. Pindak, S. Dierker, and J. F. Legrand, ESRF Newsletter, February 1994; see also Annex to the ESRF Annual Report 1993 (European Synchrotron Radiation Facility, Grenoble, 1994).

[2] M. Sutton, S. G. J. Mochrie, T. Greytak, S. E. Nagler, L. E. Berman, G. A. Held, and G. B. Stephenson, Nature (London) **352**, 608 (1991).

[3] Z. H. Cai, B. Lai, W. B. Yun, I. McNulty, K. G. Huang, and T. P. Russell, Phys. Rev. Lett. **73**, 82 (1994).

[4] J. C. Dainty, *Laser Speckle and Related Phenomena* (Springer-Verlag, New York, 1984).

[5] B. J. Berne and R. Pecora, *Dynamic Light Scattering* (Wiley, New York, 1976).

[6] P. N. Pusey, in *Photon Correlation Spectroscopy and Velocimetry,* edited by H. Z. Cummins and E. R. Pike (Plenum, New York, 1977).

[7] B. Park, G. B. Stephenson, S. M. Allen, and K. F. Ludwig, Jr., Phys. Rev. Lett. **68**, 1742 (1992).

[8] The composition was chosen to be at the maximum in $T_c$ to reduce any broadening of the transition due to composition inhomogeneity. The crystal was prepared by arc melting Fe and Al in a gettered Ar atmosphere and annealing the resulting ingot for several days at 1723 K to grow large (~10 mm) grains. Precautions were taken to avoid significant evaporation of Al during annealing. After cutting and orienting, the surface was prepared by mechanical polishing.

[9] P. C. Hohenberg and B. I. Halperin, Rev. Mod. Phys. **49**, 435 (1977).

[10] B. E. Warren, *X-ray Diffraction* (Dover, New York, 1990).

[11] E. R. Pike, in *Photon Correlation Spectroscopy and Velocimetry,* edited by H. Z. Cummins and E. R. Pike (Plenum, New York, 1977).

[12] In computing $g^{(2)}(\tau) - 1$ from the data, all time-bins were of equal size and spacing, but some were not filled due to interruptions in the data accumulation. The sums were carried out over only filled bins, and normalized to the number of summed terms. For each data set, various sizes of time-bin were investigated and found to produce very similar correlation functions.

[13] G. Grinstein (private communication).

[14] K. Binder, Z. Phys. B **43**, 119 (1981).